marine drugs

MDPI

Review

Synthetic Approaches to Zetekitoxin AB, a Potent Voltage-Gated Sodium Channel Inhibitor

Kanna Adachi, Hayate Ishizuka, Minami Odagi * and Kazuo Nagasawa *

Department of Biotechnology and Life Science, Tokyo University of Agriculture and Technology (TUAT), 2-24-16, Naka-cho, Koganei city, Tokyo 184-8588, Japan; s175364y@st.go.tuat.ac.jp (K.A.); s189783w@st.go.tuat.ac.jp (H.I.)
* Correspondence: odagi@cc.tuat.ac.jp(M.O.); knaga@cc.tuat.ac.jp (K.N.)

Received: 7 December 2019; Accepted: 24 December 2019; Published: 26 December 2019

Abstract: Voltage-gated sodium channels (Na_Vs) are membrane proteins that are involved in the generation and propagation of action potentials in neurons. Recently, the structure of a complex made of a tetrodotoxin-sensitive (TTX-s) Na_V subtype with saxitoxin (STX), a shellfish toxin, was determined. STX potently inhibits TTX-s Na_V, and is used as a biological tool to investigate the function of Na_Vs. More than 50 analogs of STX have been isolated from nature. Among them, zetekitoxin AB (ZTX) has a distinctive chemical structure, and is the most potent inhibitor of Na_Vs, including tetrodotoxin-resistant (TTX-r) Na_V. Despite intensive synthetic studies, total synthesis of ZTX has not yet been achieved. Here, we review recent efforts directed toward the total synthesis of ZTX, including syntheses of 11-saxitoxinethanoic acid (SEA), which is considered a useful synthetic model for ZTX, since it contains a key carbon–carbon bond at the C11 position.

Keywords: saxitoxin; zetekitoxin AB; voltage-gated sodium channel; guanidine alkaloid

1. Introduction

1.1. Voltage-Gated Sodium Channel Isoforms

Voltage-gated sodium channels (Na_Vs) are membrane proteins involved in neuronal excitation and transmission [1]. Ten subtypes, Na_V1.1–1.9 and Na_VX, have been identified based on sequence determination (Table 1) [2]. These subtypes can be grouped into two types depending upon their sensitivity to the pufferfish toxin, tetrodotoxin (TTX) [3–7]: tetrodotoxin-sensitive Na_Vs (TTX-s Na_Vs 1.1–1.4, 1.6, and 1.7) are significantly inhibited by TTX, while tetrodotoxin-resistant Na_Vs (TTX-r Na_Vs 1.5, 1.8, 1.9) are not [8–23]. Subtype-selective modulators of Na_Vs are required for studies to establish the biological functions of these subtypes. Some of the subtypes are also considered to be potential drug targets; for example, Na_V1.7 and 1.8 are potential targets for pain treatment [24–29]. Therefore, there is great interest in the development of drugs targeting specific subtypes [30,31].

Table 1. Isoforms of a voltage-gated sodium channel (Na_V) and their classifications.

Na_V Isoform	Primary Locations	Related Diseases	TTX IC_{50} (nM)
TTX-sensitive			
$Na_V1.1$	CNS, PNS, heart	Epilepsy	5.9
$Na_V1.2$	CNS	Epilepsy	7.8
$Na_V1.3$	Embryonic CNS, injured DRG	Nerve injury	2.0
$Na_V1.4$	Skeletal muscle	Myotonia	4.5
$Na_V1.6$	CNS, PNS, SMCs, DRG	CNS disorders	3.8
$Na_V1.7$	PNS, DRG	Pain sensation	5.5
TTX-resistant			
$Na_V1.5$	Heart, embryonic CNS	Cardiac arrhythmias	1970
$Na_V1.8$	PNS, DRG	Pain sensation	1330
$Na_V1.9$	PNS, DRG	Pain sensation	59,600

TTX: tetrodotoxin; CNS: central nervous system; PNS: peripheral nervous system; DRG: dorsal root ganglion; SMCs: smooth muscle cells.

1.2. Saxitoxin As A Na_V Modulator

Saxitoxin (STX, **1**) is a guanidine alkaloid with potent and specific inhibitory activity towards Na_Vs (Figure 1) [32,33]. It has long been known as a shellfish toxin. In 1937, Sommer and co-workers found that toxin-free bivalves, including the dinoflagellate *Gonyaulax catenella*, became poisoned in seawater, and they revealed that the real producer of STX (**1**) is algae [34,35]. Then, STX (**1**) was first isolated from Alaska butter clams by Schantz's group in 1957 [36,37]. Rapport's group subsequently isolated the same toxin from the same shellfish, and named it saxitoxin [38]. Structural elucidation was troublesome. Initially, tri- or tetracyclic structures were proposed based upon the molecular formula and the presence of two guanidines as functional groups. Finally, the structure of STX (**1**) was independently determined by the two groups by means of X-ray analysis in 1975 [39,40]. STX (**1**) consists of ten carbons, seven nitrogens, and four oxygens, and all the carbons except for C11 are connected with heteroatoms. STX (**1**) contains five- and six-membered cyclic guanidines, which have different pKa values of 8.7 and 12.4, respectively; the five-membered one is less basic, presumably due to its less planar structure [41].

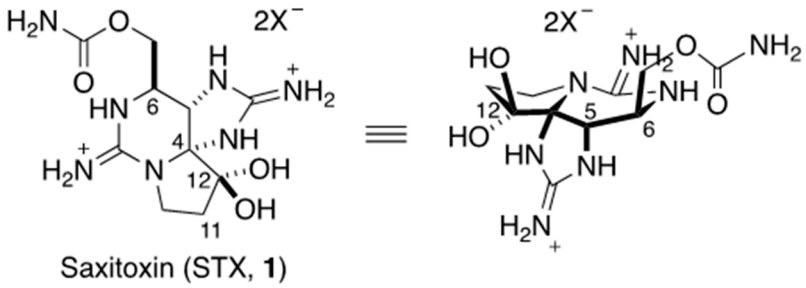

Figure 1. Structure of saxitoxin (STX, **1**).

STX (**1**) binds to the pore-forming region of the alpha-loop of Na_V and blocks the influx of sodium cation in a similar manner to tetrodotoxin (TTX) [42,43]. Recently, Yan's group determined the X-ray structure of the complexes of STX (**1**) with Na_VPas derived from American cockroach and human-derived $Na_V1.7$ by using cryoEM (Figure 2) [44,45]. They found that the carbamoyl group at C13 in STX (**1**) interacts with Gly1407 and Thr1409 in domain III, the two guanidines interact with Glu364 in domain I and Glu930 in domain II, and the geminal diol interacts with Asp1701 in domain IV. Interestingly, residues 1409 and 1410, located in the P2 loop of domain III in $Na_V1.7$, were mutated to Thr and Ile from Met and Asp, respectively, which may explain why STX (**1**) has a weaker affinity for $Na_V1.7$ compared with other subtypes (Met1409 and Asp1410 are conserved in the other subtypes of TTX-s) [46,47].

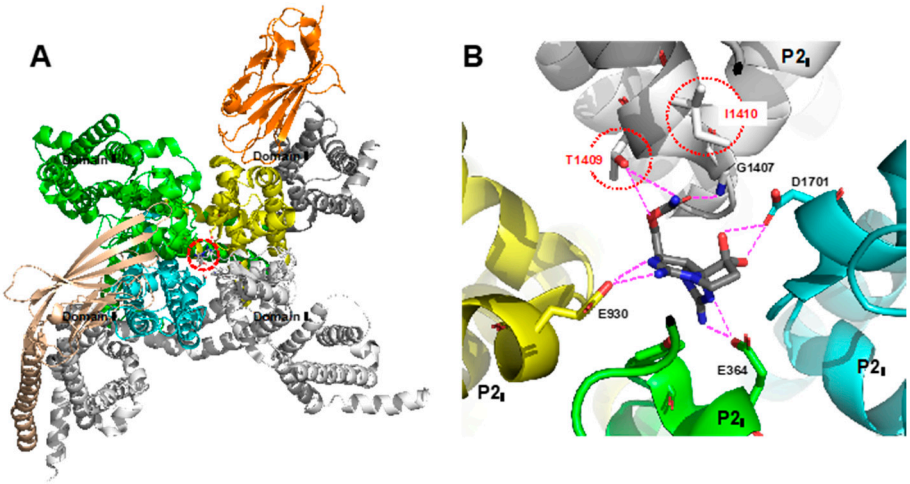

Figure 2. (**A**) Top view of the structure of the STX–$Na_V1.7$ complex. (**B**) Specific interactions in the STX–$Na_V1.7$ complex [45].

1.3. Natural Analogs of Saxitoxin, Including Zetekitoxin AB (ZTX)

To date, more than 50 kinds of natural analogs of saxitoxin have been reported, of which most are modified at N1 (R^1), C11 (i.e., R^2 and R^3), or C13 (R^4) in the common structure shown in Figure 3A [48]. For example, neosaxitoxin (neoSTX, **2**) is hydroxylated at N1, decarbamoylsaxitoxin (dcSTX, **3**) has a hydroxyl group at C13, and gonyautoxins I–III (GTX I–III, **5**–**7**, respectively) have a sulfate ester at C11; all of these analogs show similar Na_V-inhibitory activity to STX (**1**).

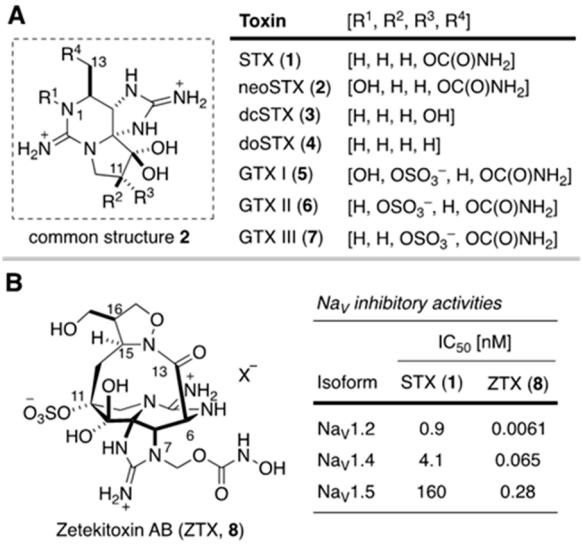

Toxin	[R^1, R^2, R^3, R^4]
STX (**1**)	[H, H, H, OC(O)NH_2]
neoSTX (**2**)	[OH, H, H, OC(O)NH_2]
dcSTX (**3**)	[H, H, H, OH]
doSTX (**4**)	[H, H, H, H]
GTX I (**5**)	[OH, OSO_3^-, H, OC(O)NH_2]
GTX II (**6**)	[H, OSO_3^-, H, OC(O)NH_2]
GTX III (**7**)	[H, H, OSO_3^-, OC(O)NH_2]

Na_V inhibitory activities

	IC_{50} [nM]	
Isoform	STX (**1**)	ZTX (**8**)
$Na_V1.2$	0.9	0.0061
$Na_V1.4$	4.1	0.065
$Na_V1.5$	160	0.28

Figure 3. (**A**) Representative STX derivatives. (**B**) Structure and Na_V-inhibitory activities of zetekitoxin AB (**8**) [49].

Among the STX (**1**) derivatives, zetekitoxin AB (ZTX, **8**) has an unusual structure [49]. ZTX (**8**) was isolated from skin of the Panamanian dart-poison frog *Atelopus zeteki* in 1969 by Mosher and co-workers [50,51]. It has extremely potent Na_V-inhibitory activity (more than 600-fold greater than that of STX (**1**)), with IC_{50} values of 6.1 pM, 65 pM, and 280 pM for $Na_V1.2$, $Na_V1.4$, and TTX-r subtype $Na_V1.5$, respectively [49]. Thus, there is great interest in the mode of action of ZTX (**8**), but studies are hampered by the fact that *Atelopus zeteki* is designated as an endangered species. Therefore, a chemical synthesis of ZTX (**8**) is needed. However, ZTX (**8**) contains a macrocyclic lactam structure in which isoxazolidine is bridged from C6 to C11, and an *N*-hydroxycarbamate is linked via a methylene group

at N7 [49]. These structural features make ZTX (**8**) synthetically challenging. So far, several synthetic approaches have been reported, but a total synthesis of **8** has not yet been achieved.

1.4. Scope of This Review

Synthetic studies of STX (**1**) and its analogs have been extensive, and several total syntheses have been achieved [52–61], as recently reviewed by Du Bois [62]. Approaches for developing of subtype-selective modulators based on the STX structure have also been explored [25,47,63–65]. However, in this review, we focus on recent synthetic work related to ZTX (**8**). As described above, ZTX (**8**) has a characteristic macrolactam structure though C6 to C11 with an isoxazolidine ring system, and is structurally quite distinct from other STX analogs. To achieve total synthesis of ZTX (**8**), two key issues must be addressed: (i) carbon–carbon bond formation at the C11 position in the STX skeleton, and (ii) macrolactam formation of the carboxylic acid at C6 with isoxazolidine nitrogen (Figure 4). Regarding the first issue, the STX derivative 11-saxitoxinethanoic acid (SEA, **9**) has been used as a synthetic model for **8**, since it also has a carbon–carbon bond at the C11 position. As for the second issue, stereoselective synthesis of disubstituted isoxazolidine and oxidation to carboxylic acid at C13, followed by amide formation with the isoxazolidine, have been examined. First, we will consider recent progress in the total synthesis of SEA (**9**).

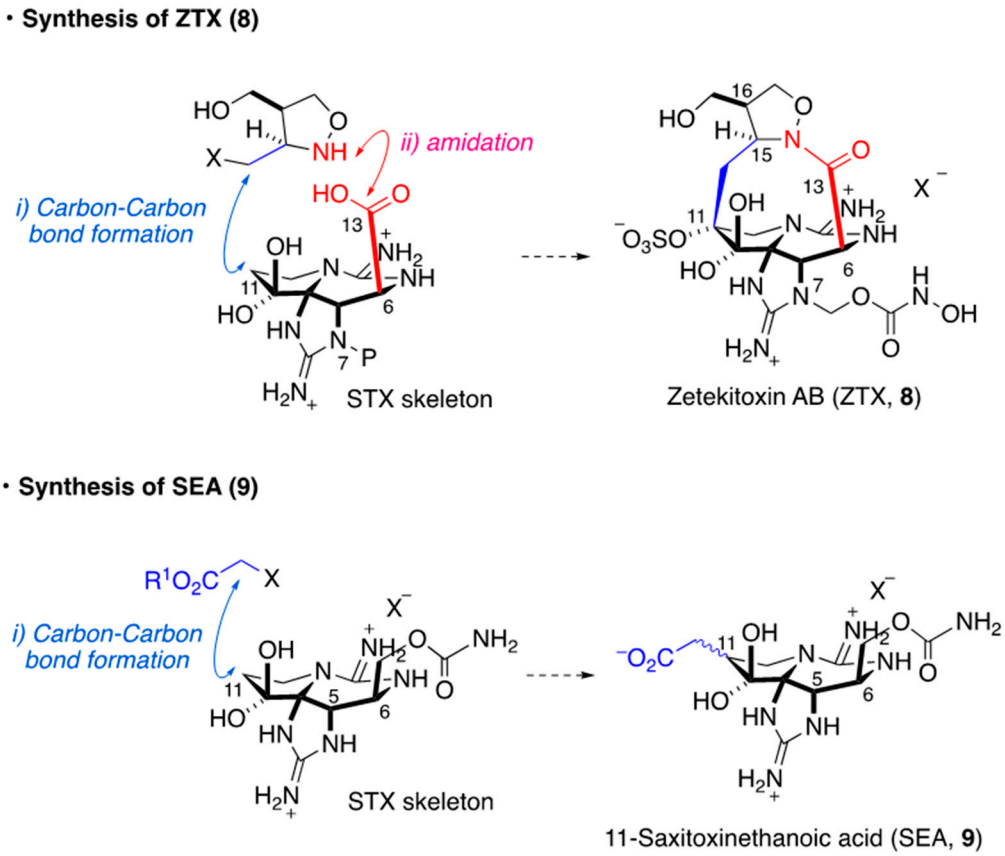

Figure 4. Key issues in the synthesis of ZTX (**8**) and 11-saxitoxinethanoic acid (SEA, **9**).

2. Development of Carbon–Carbon Linkage at C11 of STX, And Application to The Synthesis of 11-Saxitoxinethanoic Acid (SEA, 9)

The STX analog 11-saxitoxinethanoic acid (SEA, **9**) was isolated from *Atergatis floridus*, an Indo-Pacific crab from the family Xanthidae, by Onoue and co-workers (Figure 5) [66]. SEA (**9**) has an acetic acid moiety linked to C11 through a carbon–carbon bond, as seen in ZTX (**8**), and is regarded as a promising synthetic model compound for **8** in terms of construction of the carbon–carbon connection at C11.

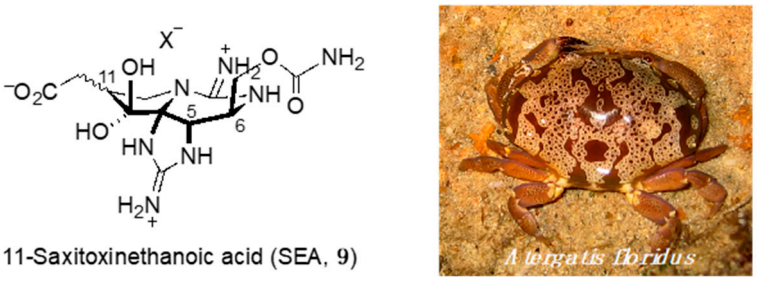

Figure 5. Structure of 11-saxitoxinethanoic acid (SEA, **9**) and illustration of the source crab species.

Recently, three total synthesis of SEA (**9**) were independently reported, including one by our group [67–69]. When **9** was first isolated, its toxicity to mice was reported to be 830 μmol/MU, which is similar to that of gonyautoxin II (GTX II, **6**) and one-third of that of STX (**1**), but no information about the Na_V-inhibitory activity was provided. After the synthesis of **9**, Du Bois and our group independently evaluated the Na_V-inhibitory activity of **9**. Nagasawa, Yotsu-Yamashita, and co-workers evaluated the Na_V-inhibitory activity of SEA (**9**) by utilizing neuroblastoma Neuro 2A cells, which is known to express Na_V1.2, 1.3, 1.4, and 1.7 [70], and found moderate inhibitory activity with an IC_{50} value of 47.0 ± 1.2 nM (Figure 6B) [67]. Du Bois and co-workers evaluated the inhibitory activity of **9** against Na_V1.4, and found that SEA (**9**) showed similar inhibitory activity to gonyautoxin III (GTX III, **7**) (**9**: IC_{50} = 17 ± 1.9 nM; GTX III (**7**): IC_{50} = 14.9 ± 2.1 nM), even though it was a diastereomeric mixture of α:β = 3:1 at C11 (Figure 6A) [68]. They suggested that the β-form of **9** binds to Na_V preferentially, and then the α-form of **9** isomerizes to the β-form, which shows a similar level of inhibitory activity to GTX III (**7**) (Figure 6C).

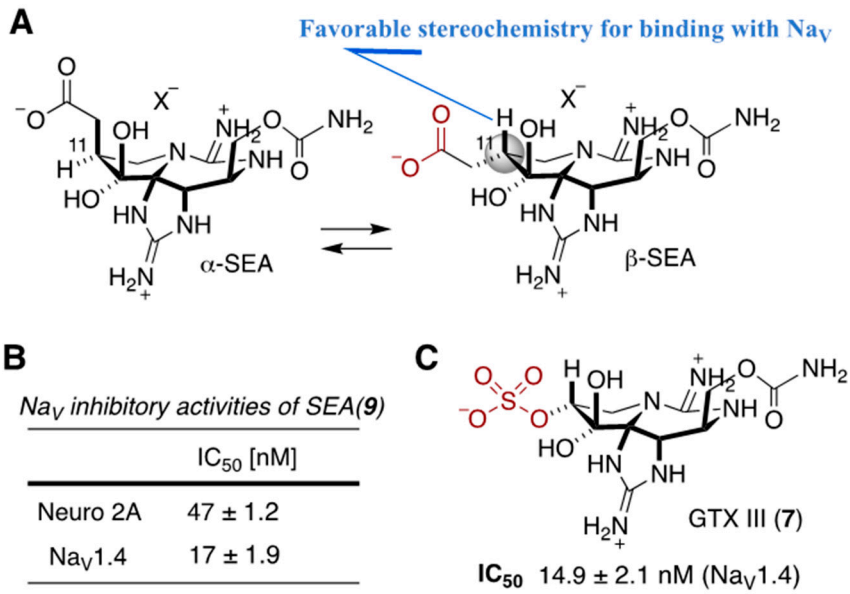

Figure 6. (**A**) Isomerization of α-SEA to β-SEA. (**B**) Na_V-inhibitory activity of SEA (**9**) [69,70]. (**C**) Structure of GTX III (**7**) and IC_{50} (Na_V1.4).

2.1. Carbon–Carbon Bond Formation at C11 by Mukaiyama Aldol Condensation Reaction, as Applied for The Synthesis of (+)-SEA by Nagasawa's Group

For the construction of a carbon–carbon bond at C11, Nagasawa and co-workers utilized ketone **10**, which was previously developed by their group [67], to install an acetic acid equivalent at C11. They firstly investigated the alkylation reaction of the enolate of ketone **10a** with alpha-halo-ethyl acetate. With various bases and halogens, the alkylation did not take place at all, and the starting ketone **10a** was recovered. Next, they investigated the Mukaiyama aldol reaction [71–73]. Thus, silyl

enol ethers **11a** and **11b** were synthesized from the ketone by reaction with *tert*-butyldimethylsilyl chloride in the presence of NaHMDS as a base. Then, the Mukaiyama aldol reaction was examined with ethyl glyoxylate under various conditions. Lewis acids, such as $TiCl_4$ or BF_3 Et_2O [74,75], removed the *tert*-butoxycarbonyl (Boc) protecting group of guanidine, and no coupling products with ethyl glyoxylate were obtained. In the case of the fluoride anion agent Bu_4NF [76], the reaction did not proceed at all. On the other hand, with anhydrous tetrabutyl bisfluorotriphenylphosphine stannate, developed by Raimundo and co-workers [77], the coupling reaction with ethyl glyoxylate proceeded very well to afford the aldol-condensation product **12a** a 96% yield (Table 2). Aromatic aldehydes were tolerated, as well as aliphatic aldehydes, and the corresponding aldol condensation products **12a–i** were obtained with 42%–80% yield. This reaction afforded mixtures of regioisomers in ratios of 5:1 to >10:1.

Table 2. Substrate scope of the Mukaiyama aldol condensation reaction of **11a** and **11b** with aldehydes.

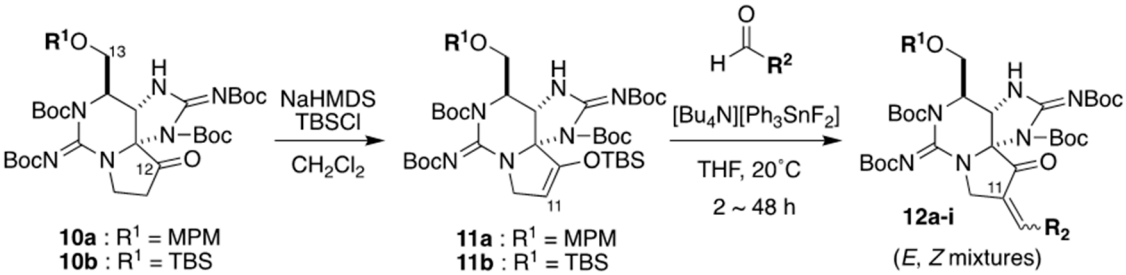

Entry.	SM	R^2	12 (*E*:*Z*) [a]	Yield (%)
1	**11a**	CO_2Et	**12a** (5:1)	96
2	**11b**	CO_2Et	**12b** (5:1)	85
3	**11a**	4-MeC_6H_4	**12c** (> 1:1)	45
4	**11a**	3-FC_6H_4	**12d** (> 10:1)	63
5	**11a**	4-ClC_6H_4	**12e** (> 10:1)	65
6	**11a**	4-$NO_2C_6H_4$	**12f** (6:1)	80
7	**11a**	2-Furyl	**12g** (> 10:1)	80
8	**11a**	C_6H_5	**12h** (> 10:1)	60
9	**11b**	C_6H_5	**12i** (*E*:*Z*) [a]	42

[a] Ration at C11 were determined by 1H NMR spectroscopy.

With the aldol condensation product **12b** in hand, Nagasawa and co-workers went on to achieve a total synthesis of (+)-SEA (**9**) for the first time (Scheme 1). Thus, selective reduction of the enone moiety in **12b** was carried out with L-selectride, and the protecting group of *tert*-butyldimethylsilyl (TBS) ether was removed with triethylamine trihydrofluoride (3HF-TEA). The resulting alcohol was reacted with trichloroisocyanate, followed by hydrolysis of the trichloroacetyl group with triethylamine in methanol to give carbamoyl **15**. After hydrolysis of ethyl ester in **15** with lithium hydroxide, the Boc group was removed with TFA to give (+)-SEA (**9**).

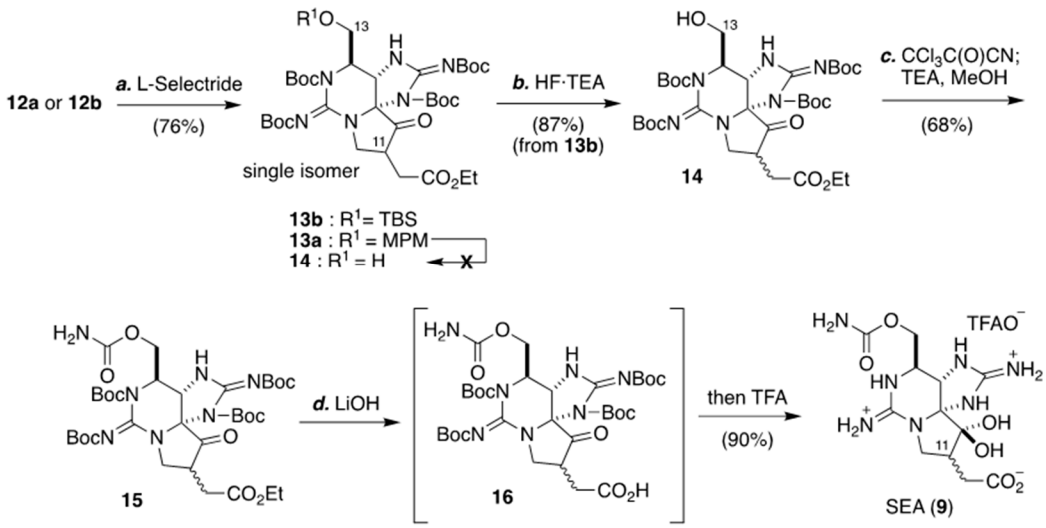

Scheme 1. Total synthesis of SEA (**9**) by Nagasawa's group.

2.2. Carbon–Carbon Bond Formation At C11 by Stille Coupling Reaction, As Applied for The Synthesis of (+)-SEA by Du Bois' Group

Another approach for the construction of the carbon–carbon bond at C11 in STX was explored by Du Bois and co-workers, who employed Stille coupling reaction conditions [68]. They firstly examined the coupling reaction of zinc enolate of ethyl acetate or the stannane enolate of ethyl acetate-type agents with vinyl halide **17**, which was prepared from **20**, developed by their group (Scheme 2), in the presence of palladium catalyst (Table 3, entries 1 and 2) [78–83]. Under the conditions examined, decomposition of the starting substrate was observed in the case of zinc agent, and no reaction occurred with the stannane agent. Then they examined the Stille coupling reaction, using vinyl stannane for the construction of the carbon–carbon bond at C11 [84]. A Stille coupling reaction of vinyl iodide **17** with tributyl(vinyl)tin was examined in the presence of a catalytic amount of $Pd(PPh_3)_4$, with CuI as an additive (a standard condition). Unfortunately, only a trace amount of the corresponding coupling product of **18c** was obtained (entry 3). Then, they changed vinyl stannane to cis-tributyl (2-ethoxyvinyl) tin, and included LiCl as an additional additive. Under these conditions, the corresponding coupling product **18d** was obtained with 67% yield (entry 4) [85,86]. Interestingly, poor reproducibility or low yield of the coupling reaction was observed when they used a highly oxidized vinyl stannane agent, tributyl(2,2-diethoxyvinyl)stannane (entry 5). This issue was successfully overcome by switching from CuI to copper(I) thiophene-2-carboxylate (CuTC), and **19** was obtained with 60% yield and with good reproducibility (entry 6) [87].

Based upon the Stille coupling strategy, Du Bois and co-workers achieved a total synthesis of SEA (**9**), as shown in Scheme 2, including the synthesis of vinyl halide **17** as a substrate for the Stille coupling reaction. Firstly, vinyl halide **17** was synthesized from **20** via Mislow–Evans [2,3] rearrangement: bisguanidine **20** was converted to *N*,*S*-acetal **21** by reaction with benzenethiol in the presence of $BF_3{\cdot}Et_2O$ with 84% yield. Upon treatment of **21** with urea–hydrogen peroxide (UHP), the Mislow–Evans [2,3] rearrangement reaction [88,89] took place under heating in the presence of sodium benzenthiolate, and allylic alcohol **23** was obtained with 81% yield in two steps. After oxidation of the alcohol with Dess–Martin periodinate, the resulting enone **24** was reacted with iodine in the presence of pyridine to give vinyl iodide **17** [90,91], which was further elaborated to **19** by Stille coupling reaction with **25** with 60% yield. Then, the double bond in enone **19** was hydrogenated under high pressure in the presence of Crabtree catalyst **26**. Deprotection of the *tert*-butyldiphenylchlorosilane (TBDPS) ether in **27** with tetrabutylammonium (TBAF) was followed by installation of a carbamoyl group on the resulting hydroxyl group. Finally, deprotection of Tces and Troc and hydrolysis of the ester group were carried out to give (+)-SEA (**9**).

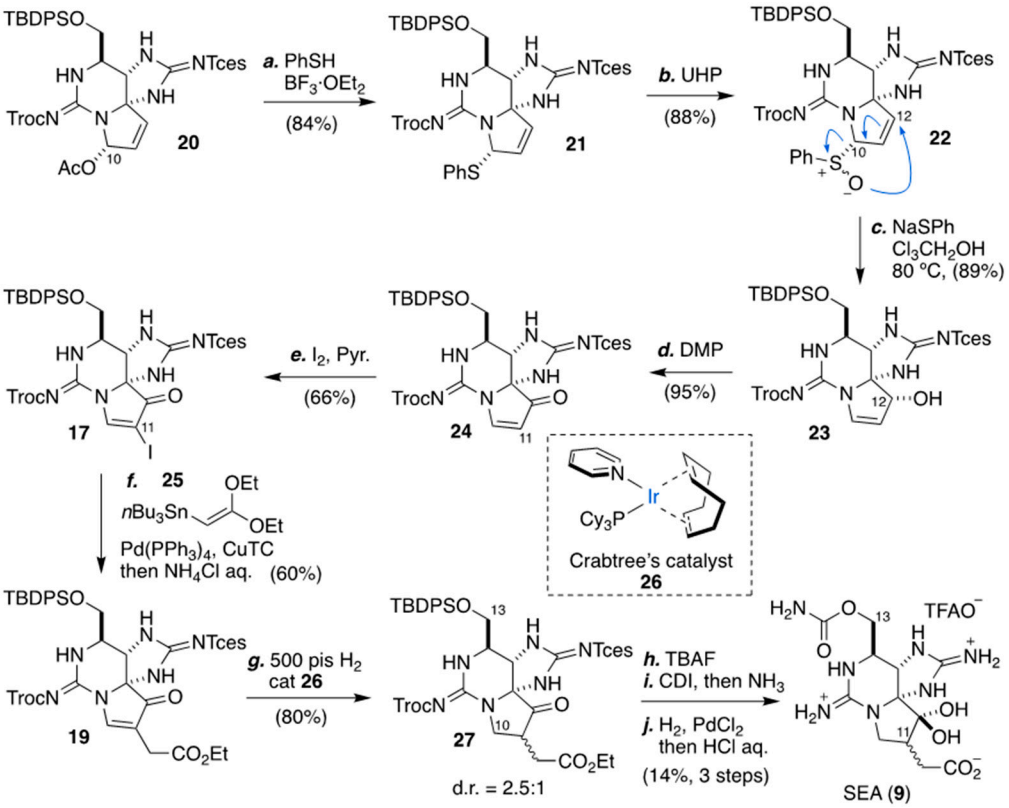

Scheme 2. Introduction of substituent at C11 by Stille coupling, leading to total synthesis of (+)-SEA (**9**) by Du Bois' group.

Table 3. Stille-based cross-coupling conditions with iodoenaminone **17**.

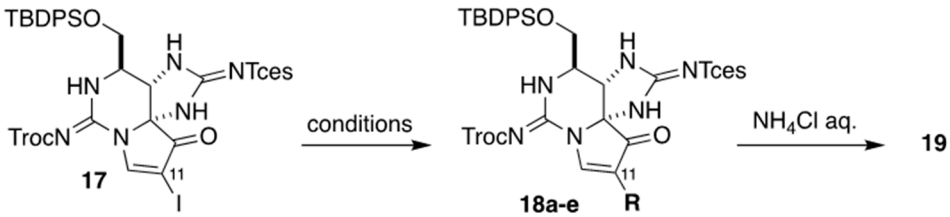

Entry	Conditions	R	Result
1	$CH_2C(OZnBr)OtBu$, $Pd_2(dba)_3$/dppf, THF	CH_2CO_2tBu	**18a** (decomp.)
2	$CH_2C(OSnnBu_3)OEt$, $PdCl_2(P(o\text{-}tol)_3)_2$, CuF_2	CH_2CO_2Et	**18b** (N.R.)
3	$nBu_3SnCH{=}CH_2$, $Pd(PPh_3)_4$, CuI	$CH{=}CH_2$	**18c** (< 5%)
4	$nBu_3SnCH{=}CH(OEt)$, $Pd(PPh_3)_4$, CuCl, LiCl, THF	CH=CH(OEt)	**18d** (67%)
5	$nBu_3SnCH{=}C(OEt)_2$, $Pd(PPh_3)_4$, CuCl, LiCl, THF	$CH{=}C(OEt)_2$	**19** (0–40%)
6	$nBu_3SnCH{=}C(OEt)_2$, $Pd(PPh_3)_4$, CuTC, THF	$CH{=}C(OEt)_2$	**19** (60%)

CuTC = Copper (I) thiophene-2-carboxylate.

2.3. Carbon–Carbon Bond Formation at C11 by C-Alkylation, As Applied for The Synthesis of (+)-SEA by Looper's Group

In 2019, Looper and co-workers successfully constructed a carbon–carbon bond at C11 in STX, and reported a total synthesis of SEA (**9**) [69]. They initially examined C-alkylation with ketone **28** and electrophiles in the presence of variety of bases, such as lithium bis(trimethylsilyi)amide (LHMDS), lithium diisopropyl amide (LDA), potassium bis(trimethylsilyi)amide (KHMDS) and sodium bis(trimethylsilyi)amide (NaHMDS). In addition, they examined various electrophiles (haloacetates, allylic halides, and propargylic halides), but no reaction took place, as Nagasawa and co-workers had found (Scheme 3) [67].

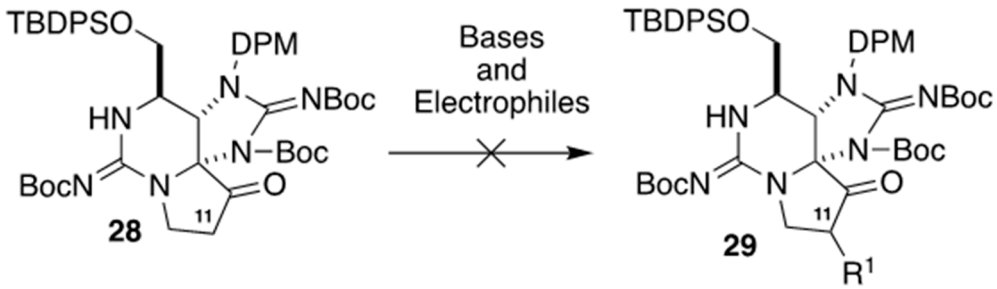

Scheme 3. Examination of carbon–carbon bond construction at C11 by alkylation with ketone **28** in the presence of bases.

On the other hand, they found that C-alkylation took place upon reaction of ketone **28** and *tert*-butyl bromoacetate via the generation of zinc enolate by reaction with LiHMDS in the presence of Et_2Zn, affording a mixture of **29a** and its Boc-deprotected derivative **29b** with 60% yield (based on the starting material) (Scheme 4). By means of this alkylation strategy, they succeeded in synthesizing ZTX (**9**) as follows. Deprotection of TBDPS ether in **29** with TBAF followed by carbamoylation of the resulting alcohol resulted in **30**. Finally, total synthesis of SEA (**9**) was achieved by reaction with TFA to hydrolyze the ester and deprotect the Boc and DPM groups.

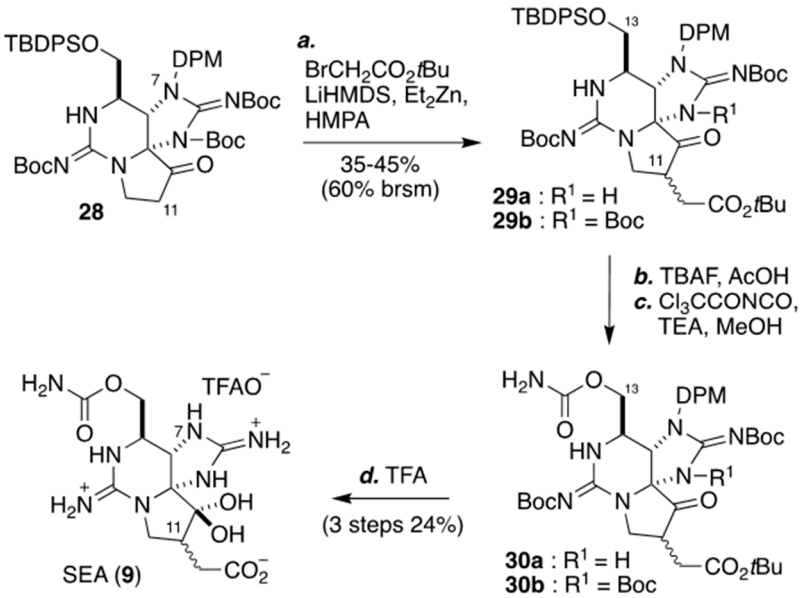

Scheme 4. Carbon–carbon bond formation at C11 by C-alkylation, and total synthesis of (+)-SEA (**9**) by Looper's group.

2.4. Na_V-Inhibitory Activity of Synthesized, C11-Substituted Saxitoxin Analogs

Based on the method described above for constructing a carbon–carbon bond at C11 in STX, Nagasawa and co-workers synthesized a series of STX analogs bearing substituents at C11, and evaluated the Na_V-inhibitory activity of these analogs at the cellular level [67].

Beside SEA (**9**), they synthesized dicarbamoyl SEA (dcSEA, **31**), 11-saxitoxin ethyl ethanoate (SEE, **32**), and 11-benzylidene STX (**33a**), and evaluated their Na_V-inhibitory activity in mouse neuroblastoma Neuro 2A cells, which is known to express $Na_V1.2$, 1.3, 1.4, and 1.7 [70]. SEA (**9**) showed potent inhibitory activity with an IC_{50} value of 47 ± 12 nM, which is twice as potent as decarbamoyl saxitoxin (dcSTX (**3**), IC_{50} = 89 ± 36 M) (Figure 7, Table 4). The dcSEA (**31**) and SEE (**32**) showed IC_{50} values of 5700 ± 3.1 and 185 ± 74 nM, respectively. Interestingly, 11-benzylidene STX (**33a**) was a potent inhibitor, with an IC_{50} value of 16.0 ± 6.9 nM. Although the inhibition mode of **33a** has not been clarified yet, the non-hydrated keto group at C12 in **33** might bind efficiently with Na_V, resulting in potent inhibitory activity.

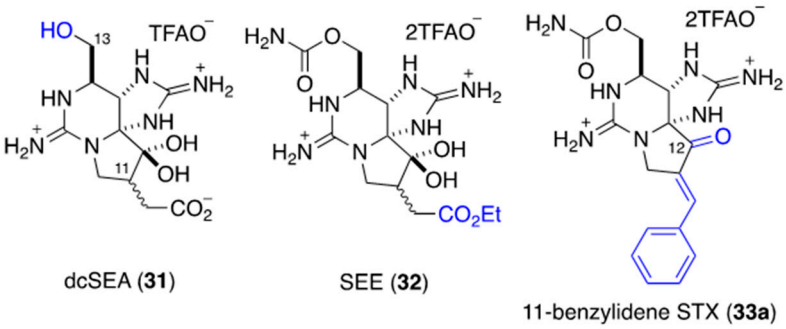

Figure 7. Structures of 9, 31, 32, and 33a.

Table 4. Na_V-inhibitory activity of **9**, **31**, **32**, and **33a** in a cell-based assay with Neuro 2A cells.

Compound	IC_{50} (mean ± SD) (nM)	n
dcSTX (**3**)	89 ± 36	3
SEA (**9**)	47 ± 12	3
dcSEA (**31**)	5700 ± 3.1	3
SEE (**32**)	185 ± 74	4
11-benzylidene STX (**33a**)	16 ± 6.9	5

Next, they further synthesized 11-substituted STX analogs **33b**–**f**, and elucidated their subtype selectivity towards $Na_V1.2$, 1.5, and 1.7, using the whole-cell patch-clamp recording method (Figure 8, Table 5) [92]. They found that 11-fluorobenzylidene STX (**33c**) showed selective and potent inhibitory activity against $Na_V1.2$ (IC_{50} = 7.7 ± 1.6 nM), compared to the other subtypes tested. 11-Benzylidene STX (**33a**) and 11- nitrobenzylidene STX (**33d**) showed potent inhibitory activity against $Na_V1.5$, with IC_{50} values of 94.1 ± 12.0 nM and 50.9 ± 7.8 nM, respectively. These compounds are the most potent TTX-r modulators among STX derivatives so far reported, except for ZTX (**8**) [49].

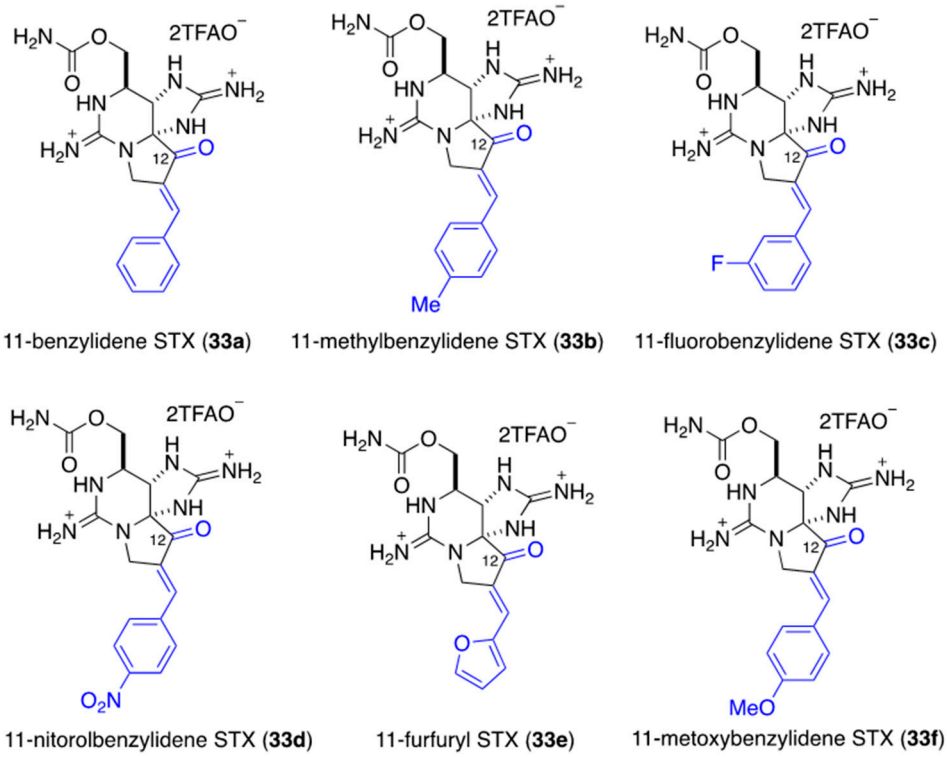

Figure 8. Structures of 33a–f.

Table 5. Na_V-inhibitory activities of **33a–f**, using whole-cell, patch-clamp recording.

Compound	$hNa_V1.2$	$hNa_V1.5$	$hNa_V1.7$
11-benzylidene STX (**33a**)	5.2 ± 6.0	94.1 ± 12.0	124.1 ± 20.6
11-methylbenzylidene STX (**33b**)	22.9 ± 8.6	>300	>300
11-fluorobenzylidene STX (**33c**)	7.7 ± 1.6	>300	>300
11-nitrobenzylidene STX (**33d**)	8.79 ± 0.96	50.9 ± 7.8	>300
11-furfuryl STX (**33e**)	542.7 ± 65.7	>300	>300
11-metoxybenzylidene STX (**33f**)	45.0 ±2.72	>300	>300

IC_{50} (mean ± SD) (nM).

3. Stereoselective Synthesis of The Isoxazolidine Moiety of ZTX (8), And Its Introduction at C13 in A Model Compound

As described in the introduction, ZTX (**8**) has a characteristic macrolactam structure from C6 to C11, involving an isoxazolidine ring system. Thus, stereoselective synthesis of the di-substituted isoxazolidine unit in ZTX (**8**) has been examined. In the paper reporting the isolation of **8** in 2004, the amide carbonyl group in ZTX (**8**) at C13 appeared at 156.5 ppm in the ^{13}C nuclear magnetic resonance (NMR) spectrum, which is a higher chemical shift compared to other amide carbonyls [49]. This interesting observation might be attributed to the unusual macrolactam structure in ZTX (**8**), and synthetic studies of model compounds have been carried out to understand the origin of this unusual chemical shift. In the following section, we discuss the stereoselective isoxazolidine syntheses reported by Nishikawa's [93] and Lopper's groups [94].

3.1. Synthesis of The Isoxazolidine Part of Zetekitoxin (8) from D-ribose by Nishikawa And Co-workers

In 2009, Nishikawa and co-workers reported the stereoselective synthesis of isoxazolidine **42** from D-ribose (**34**) (Scheme 5) [93]. They firstly synthesized nitroolefin **36** from aldehyde **35**, which was derived from D-ribose (**34**) by means of a Henry reaction followed by dehydration with mesylation. After reduction of the double bond in **36** with $NaBH_4$, the resulting nitroalkane **37** was treated with Boc_2O to produce dihydrooxazole **39a** and **39b** with 86% yield, as a diastereomeric mixture at C16 in a ratio of 3:1. In this reaction, nitrile oxide **38** was generated first, and a 1,3-dipolar cyclization reaction occurred simultaneously. The major transition state model is shown in Scheme 5. The major diastereomer **39a** was reduced stereoselectively with $NaBH_3CN$ to isoxazolidine **40**. After acetylation of the amine in **40**, isoxazolidine **42**, which has the same stereochemistry as ZTX at C15 and C16, was obtained in three steps: (1) deprotection of acetonide with TFA, (2) oxidative cleavage of diol with $NaIO_4$, and (3) reduction of the resulting aldehyde with $NaBH_4$.

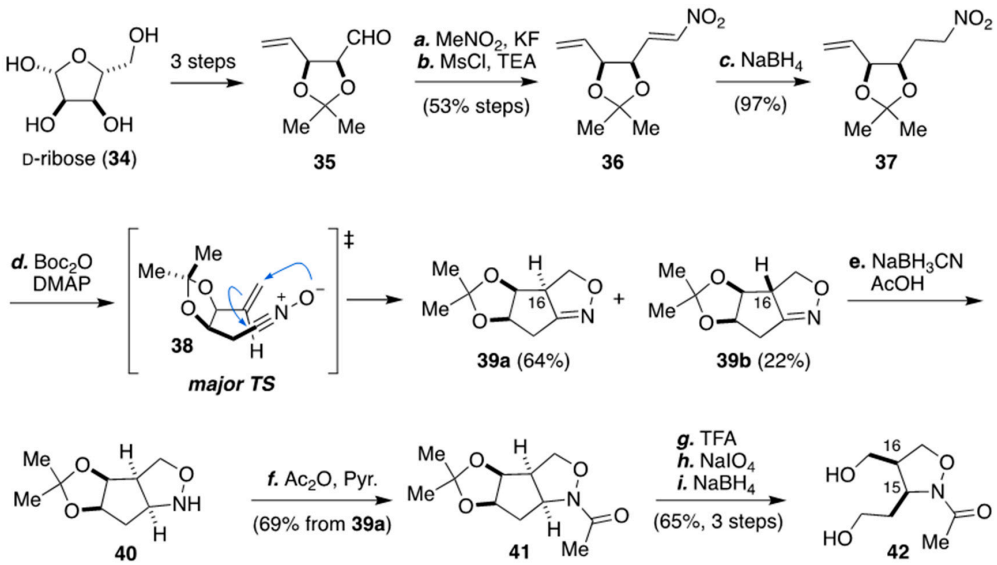

Scheme 5. Synthesis of the isoxazolidine **42** by Nishikawa's group.

3.2. Stereoselective Synthesis of The Isoxazolidine Part from Methyl α-D-glucopyranoside by Lopper and Co-Workers

In 2015, Lopper and co-workers reported a synthesis of isoxazolidine **59** (Scheme 6) [94]. Aldehyde **45** was synthesized from commercially available methyl α-D-glucopyranoside (**43**) by the iodination of **44** with iodine and PPh_3, acetylation of the hydroxyl group, and reductive cleavage of the pyran ring with zinc in acetic acid [95]. Then, intramolecular 1,3-dipolar reaction of the terminal olefin with nitrone, which was generated from aldehyde **45** by reaction with hydroxylamine **46**, took place stereoselectively to afford **48** via **47** with 52% yield. After deprotection of acetate in **48** with sodium methoxide [96,97], the resulting triol **49** was treated with $NaOI_4$ followed by $LiAlH_4$ to give diol **51** with 70% yield in two steps [98,99]. The isoxazolidine synthon **59** in ZTX (**8**) was synthesized from diol **51** in seven steps by selective functionalization of the two hydroxyl groups, followed by *N*-acylation.

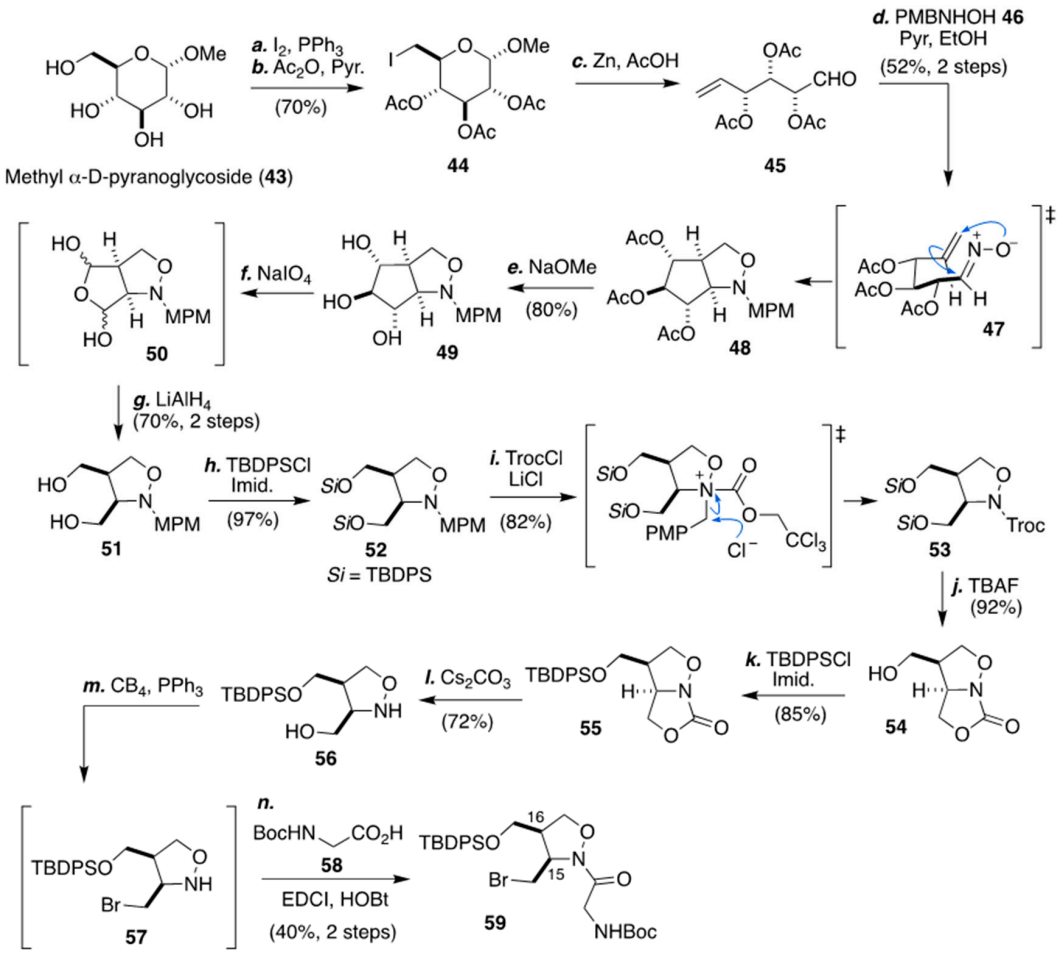

Scheme 6. Synthesis of *N*-acyl isoxazolidine **59** by Looper's group.

3.3. Comparison of the Chemical Shift at C13 in Zetekitoxin (8) with Those in Some Synthetic Models

As discussed above, the ^{13}C NMR chemical shift of the carbonyl group at C13 in ZTX (**8**) has been observed at 156.5 ppm [49], which is a higher value compared with usual amide carbonyl groups (170–175 ppm). To address the issue, Nishikawa's and Looper's groups independently examined the ^{13}C chemical shifts of the carbonyl group at C13 in some model compounds (Figure 9) [93,94]. Simple N-acyl isoxazolidine models **60**, **42**, and **59** showed chemical shifts of 171.0, 172.7, 171.0 ppm, respectively, which are quite similar to those of regular cyclic *N*-acyl amides. However, model compounds **61**–**63** bearing alpha-guanidinoacetyl amide groups showed chemical shifts of 166.0, 168.3, and 167.0 ppm, respectively, being shifted ca. 5 ppm upfield compared to the other simple models.

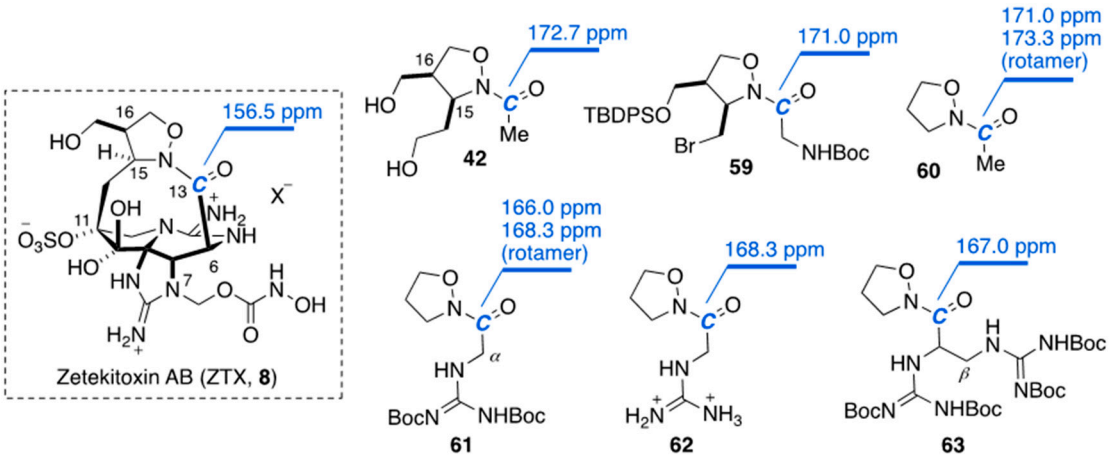

Figure 9. ^{13}C-NMR chemical shifts of ZTX (**8**) and model compounds.

Nagasawa and co-workers examined the chemical shift at C13 of **70**, which has an STX skeleton; its synthesis is depicted in Scheme 7 [100]. They firstly aimed to obtain carboxylic acid **66** from alcohol **64** by oxidation. They examined various oxidants and conditions, but it appeared that the hydroxyl group in **64** was unreactive due to its axial orientation, and no reaction occurred, or unexpected side reactions proceeded. Finally, they found that 2-azaadamantane *N*-oxyl (AZADO)–NaClO and $NaClO_2$ [101,102] were effective, resulting in carboxylic acid **66**, which was obtained with 79% yield after $TMSCHN_2$ treatment of the crude carboxylic acid **66** to hydrolyze the methyl ester **67**. Condensation of carboxylic acid **66** with isoxazolidine **40** [93] in the presence of 4-(4, 6- dimethoxy-1,3,5-triazin-2-yl)-4-methylmorpholinium chloride (DMT-MM,**68**) [103], followed by deprotection of the Boc group and acetal with TFA, gave amide **70** in 98% yield. Unfortunately, the chemical shift of the carbonyl group in **70** was observed at 166.1 ppm, slightly higher than that of **62** or **63**, but still lower than that of ZTX (**8**). The chemical shift in ZTX (**8**) may reflect the characteristic spatial structure associated with the presence of the macrolactam moiety.

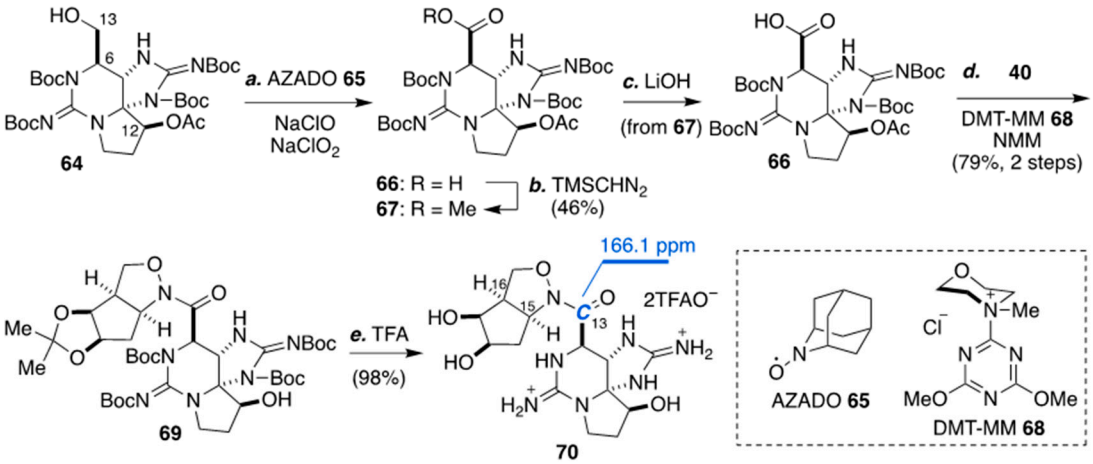

Scheme 7. Oxidation at C13 and introduction of the isoxazolidine motif.

4. Synthesis of The Characteristic Macrocyclic Structure of ZTX (8) by Looper's Group

Looper and co-workers have reported macrocyclic compound **72** as a model for ZTX (**8**) (Scheme 8) [71]. After deprotection of the TBDPS ether group at C13 with TBAF, the resulting alcohol was reacted with iodoacetic acid in the presence of 1-(3-dimethylaminopropyl)-3-ethylcarbodiimide (EDC) and N,N-dimethyl-4-aminopyridine (DMAP) to give iodoester **71** with 58% yield. When iodoester **71** was treated with a strong base, *tert*-butylimino-tri(pyrrolidino)phosphorane (BTPP), intramolecular alkylation proceeded at C11, and the corresponding macrolactone **72** was obtained

in 48% yield. It should be possible to construct the macrolactam structure of **8** via a similar strategy, and this should also resolve the chemical shift issue in ZTX (**8**).

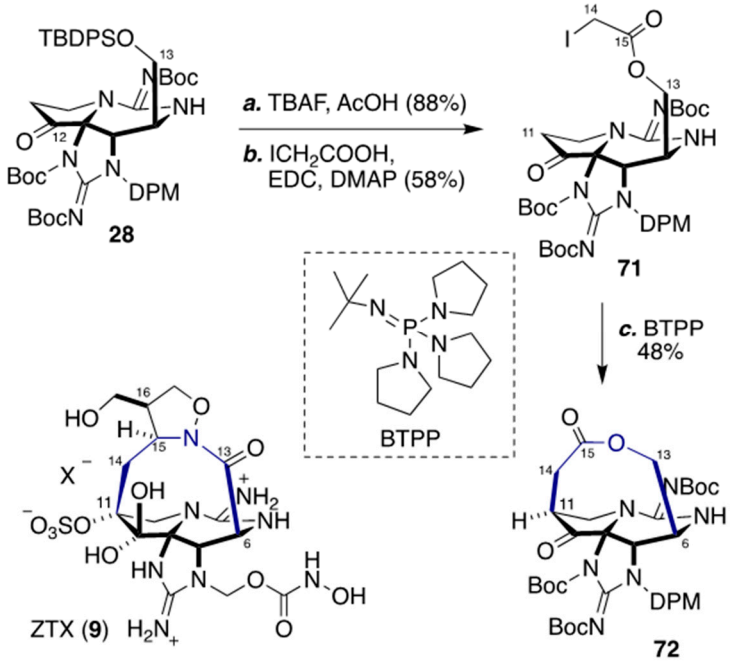

Scheme 8. Synthesis of macrolactone **72** via intramolecular alkylation by Looper's group.

5. Conclusions

Here, we have reviewed recent progress towards the total synthesis of zetekitoxin AB (**8**, ZTX). Although this goal still remains elusive, there have been some significant synthetic advances in the construction of characteristic structures of ZTX, such as (i) the carbon–carbon bond at C11 in the STX structure, (ii) stereoselective construction of the substituted isoxazolidine moiety at C15 and C16, and (iii) the macrocyclic structure from C6 to C11. Since ZTX has potent inhibitory activity, even towards tetrodotoxin-resistant (TTX-r) Na_Vs, a total synthesis of ZTX and its analogs is expected to provide useful tools for chemical biological studies of Na_Vs, overcoming the severely restricted availability of natural ZTX.

Author Contributions: Conceived and designed the story of manuscript, K.N.; writing–original draft preparation, K.N. and M.O.; writing—review and editing, K.A., H.I., M.O. All authors have read and agreed to the published version of the manuscript.

Funding: This research was funded by Grants-in-Aid for Scientific Research on Innovative Areas "Middle Molecular Strategy" (18H04387 to K.N.), Grants-in-Aid for Scientific Research (B) (JP26282214 to K.N.), and the A3-foresight program. M.O. thanks the Japan Society for the Promotion of Science (JSPS), KAKENHI Grant Number 18K14210. This work was inspired by the international and interdisciplinary environment of the JSPS Asian CORE Program of ACBI (Asian Chemical Biology Initiative).

Acknowledgments: K.A. thanks SUNBOR for providing a scholarship.

Conflicts of Interest: The authors declare no conflict of interest.

References

1. Hodgkin, A.L.; Huxley, A.F. A quantitative description of membrane current and its application to conduction and excitation in nerve. *J. Physiol.* **1952**, *117*, 500–544. [CrossRef] [PubMed]
2. Goldin, A.L.; Barchi, R.L.; Caldwell, J.H.; Hofmann, F.; Howe, J.R.; Hunter, J.C.; Kallen, R.G.; Mandel, G.; Meisler, M.H.; Netter, Y.B.; et al. Nomenclature of voltage-gated sodium channels. *Neuron* **2000**, *28*, 365–368. [CrossRef]
3. Narahashi, T. Tetrodotoxin. *Proc. Jpn. Acad. Ser. B* **2008**, *84*, 147–154. [CrossRef] [PubMed]

4. Nishikawa, T.; Isobe, M. Synthesis of Tetrodotoxin, a Classic but Still Fascinating Natural Product. *Chem. Rec.* **2013**, *13*, 286–302. [CrossRef]
5. Moczydlowski, E.G. The molecular mystique of tetrodotoxin. *Toxicon* **2013**, *63*, 165–183. [CrossRef]
6. Fozzard, H.A.; Lipkind, G.M. The Tetrodotoxin Binding Site Is within the Outer Vestibule of the Sodium Channel. *Mar. Drugs* **2010**, *8*, 219–234. [CrossRef]
7. Lee, C.H.; Ruben, P.C. Interaction between voltage-gated sodium channels and the neurotoxin, tetrodotoxin. *Channels* **2008**, *2*, 407–412. [CrossRef]
8. Clare, J.J.; Tate, S.N.; Nobbs, M.; Romanos, M.A. Voltage-gated sodium channels as therapeutic targets. *Drug Discov. Today* **2000**, *5*, 506–520. [CrossRef]
9. Noda, M.; Ikeda, T.; Kayano, T.; Suzuki, H.; Takeshima, H.; Kurasaki, M.; Takahashi, H.; Numa, S. Existence of distinct sodium channel messenger RNAs in rat brain. *Nature* **1986**, *320*, 188–192. [CrossRef]
10. Meadows, L.S.; Chen, Y.H.; Powell, A.J.; Clare, J.J.; Ragsdale, D.S. Functional modulation of human brain $Na_V1.3$ sodium channels, expressed in mammalian cells, by auxiliary beta 1, beta 2 and beta 3 subunits. *Neuroscience* **2002**, *114*, 745–753. [CrossRef]
11. Trimmer, J.S.; Cooperman, S.S.; Tomiko, S.A.; Zhou, J.; Crean, S.M.; Boyle, M.B.; Kallen, R.G.; Sheng, Z.; Barchi, R.L.; Sigworth, F.J. Primary structure and functional expression of a mammalian skeletal muscle sodium channel. *Neuron* **1989**, *3*, 33–49. [CrossRef]
12. Chahine, M.; Bennett, P.B.; George, A.L., Jr.; Horn, R. Functional expression and properties of the human skeletal muscle sodium channel. *Pflug. Arch. Eur. J. Physiol.* **1994**, *427*, 136–142. [CrossRef] [PubMed]
13. Dietrich, P.S.; McGivern, J.G.; Delgado, S.G.; Koch, B.D.; Eglen, R.M.; Hunter, J.C.; Sangameswaran, L. Functional analysis of a voltage-gated sodium channel and its splice variant from rat dorsal root ganglia. *J. Neurochem.* **1998**, *70*, 2262–2272. [CrossRef] [PubMed]
14. Smith, M.R.; Smith, R.D.; Plummer, N.W.; Meisler, M.H.; Goldin, A.L. Functional Analysis of the Mouse Scn8a Sodium Channel. *J. Neurosci.* **1998**, *18*, 6093–6102. [CrossRef] [PubMed]
15. Klugbauer, N.; Lacinova, L.; Flockerzi, V.; Hofmann, F. Structure and functional expression of a new member of the tetrodotoxin-sensitive voltage-activated sodium channel family from human neuroendocrine cells. *EMBO J.* **1995**, *14*, 1084–1090. [CrossRef] [PubMed]
16. Cummins, T.R.; Howe, J.R.; Waxman, S.G. Slow Closed-State Inactivation: A Novel Mechanism Underlying Ramp Currents in Cells Expressing the hNE/PN1 Sodium Channel. *J. Neurosci.* **1998**, *18*, 9607–9619. [CrossRef]
17. Sangameswaran, L.; Fish, L.M.; Koch, B.D.; Rabert, D.K.; Delgado, S.G.; Ilnicka, M.; Jakeman, L.B.; Novakovic, S.; Wong, K.; Sze, P.; et al. A Novel Tetrodotoxin-sensitive, Voltage-gated Sodium Channel Expressed in Rat and Human Dorsal Root Ganglia. *J. Biol. Chem.* **1997**, *272*, 14805–14809. [CrossRef]
18. Santarelli, V.P.; Eastwood, A.L.; Dougherty, D.A.; Horn, R.; Ahern, C.A. A cation-pi interaction discriminates among sodium channels that are either sensitive or resistant to tetrodotoxin block. *J. Biol. Chem.* **2007**, *282*, 8044–8051. [CrossRef]
19. Satin, J.; Kyle, J.W.; Chen, M.; Bell, P.; Cribbs, L.L.; Fozzard, H.A.; Rogart, R.B. A Mutant of TTX-Resistant Cardiac Sodium Channels with TTX-Sensitive Properties. *Science* **1992**, *256*, 1202–1205. [CrossRef]
20. Sangameswaran, L.; Delgado, S.G.; Fish, L.M.; Koch, B.D.; Jakeman, L.B.; Stewart, G.R.; Sze, P.; Hunter, J.C.; Eglen, R.M.; Herman, R.C. Structure and Function of a Novel Voltage-gated, Tetrodotoxin-resistant Sodium Channel Specific to Sensory Neurons. *J. Biol. Chem.* **1996**, *271*, 5953–5956. [CrossRef]
21. Akopian, A.N.; Sivilotti, L.; Wood, J.N. A tetrodotoxin-resistant voltage-gated sodium channel expressed by sensory neurons. *Nature* **1996**, *379*, 257–262. [CrossRef] [PubMed]
22. Dib-Hajj, S.D.; Tyrrell, L.; Black, J.A.; Waxman, S.G. NaN, a novel voltage-gated Na channel, is expressed preferentially in peripheral sensory neurons and down-regulated after axotomy. *Proc. Natl. Acad. Sci. USA* **1998**, *95*, 8963–8968. [CrossRef] [PubMed]
23. Dib-Hajj, S.; Black, J.A.; Cummins, T.R.; Waxman, S.G. NaN/$Na_V1.9$: A sodium channel with unique properties. *Trends Neurosci.* **2002**, *25*, 253–259. [CrossRef]
24. McKerrall, S.J.; Sutherlin, D.P. $Na_V1.7$ inhibitors for the treatment of chronic pain. *Bioorg. Med. Chem. Lett.* **2018**, *28*, 3141–3149. [CrossRef] [PubMed]
25. Mulcahy, J.V.; Pajouhesh, H.; Beckley, J.T.; Delwig, A.; Du Bois, J.; Hunter, J.C. Challenges and Opportunities for Therapeutics Targeting the Voltage-Gated Sodium Channel Isoform $Na_V1.7$. *J. Med. Chem.* **2019**, *62*, 8695–8710. [CrossRef] [PubMed]

26. Bagal, S.K.; Kemp, M.L.; Bungay, P.J.; Hay, T.L.; Murata, Y.; Payne, C.E.; Stevens, E.B.; Brown, A.; Blakemore, D.C.; Corbett, M.S.; et al. Discovery and optimisation of potent and highly subtype selective $Na_V1.8$ inhibitors with reduced cardiovascular liabilities. *Med. Chem. Comm.* **2016**, *7*, 1925–1931. [CrossRef]
27. Kort, M.E.; Atkinson, R.N.; Thomas, J.B.; Drizin, I.; Johnson, M.S.; Secrest, M.A.; Gregg, R.J.; Scanio, M.J.; Shi, L.; Hakeem, A.H.; et al. Subtype-selective $Na_V1.8$ sodium channel blockers: Identification of potent, orally active nicotinamide derivatives. *Bioorg. Med. Chem. Let.* **2010**, *20*, 6812–6815. [CrossRef]
28. Jarvis, M.F.; Honore, P.; Shieh, C.C.; Chapman, M.; Joshi, S.; Zhang, X.F.; Kort, M.; Carroll, W.; Marron, B.; Atkinson, R.; et al. A-803467, a potent and selective $Na_V1.8$ sodium channel blocker, attenuates neuropathic and inflammatory pain in the rat. *Proc. Natl. Acad. Sci. USA* **2007**, *104*, 8520–8525. [CrossRef]
29. Kort, M.E.; Drizin, I.; Gregg, R.J.; Scanio, M.J.; Shi, L.; Gross, M.F.; Atkinson, R.N.; Johnson, M.S.; Pacofsky, G.J.; Thomas, J.B.; et al. Discovery and biological evaluation of 5-aryl-2-furfuramides, potent and selective blockers of the $Na_V1.8$ sodium channel with efficacy in models of neuropathic and inflammatory pain. *J. Med. Chem.* **2008**, *51*, 407–416. [CrossRef]
30. Priest, B.T.; Kaczorowski, G.J. Subtype-selective sodium channel blockers promise a new era of pain research. *Proc. Natl. Acad. Sci. USA* **2007**, *104*, 8205–8206. [CrossRef]
31. England, S.; de Groot, M.J. Subtype-selective targeting of voltage-gated sodium channels. *Br. J. Pharm.* **2009**, *158*, 1413–1425. [CrossRef] [PubMed]
32. Llewellyn, L.E. Saxitoxin, a toxic marine natural product that targets a multitude of receptors. *Nat. Prod. Rep.* **2006**, *23*, 200–222. [CrossRef] [PubMed]
33. Cusick, K.D.; Sayler, G.S. An Overview on the Marine Neurotoxin, Saxitoxin: Genetics, Molecular Targets, Methods of Detection and Ecological Functions. *Mar. Drugs* **2013**, *11*, 991–1018. [CrossRef] [PubMed]
34. Sommer, H.; Meyer, G.F. Paralytic shellfish poisoning. *Arch. Pathol.* **1937**, *24*, 560–598.
35. Sommer, H.; Whedon, W.F.; Kofoid, C.A.; Strohler, R. Relation of paralytic shellfish poison to certain plankton organisms of the genus Gonyaulax. *Arch. Pathol.* **1937**, *24*, 537–559.
36. Schantz, E.J.; Mold, J.D.; Stanger, D.W.; Shavel, J.; Riel, F.J.; Bowden, J.P.; Lynch, J.M.; Wyler, R.S.; Riegel, B.; Sommer, H. Paralytic Shellfish Poison. VI. A Procedure for the Isolation and Purification of the Poison from Toxic Clam and Mussel Tissues. *J. Am. Chem. Soc.* **1957**, *79*, 5230–5235. [CrossRef]
37. Mold, J.D.; Bowden, J.P.; Stanger, D.W.; Maurer, J.E.; Lynch, J.M.; Wyler, R.S.; Schantz, E.J.; Riegel, B. Paralytic Shellfish Poison. VII. Evidence for the Purity of the Poison Isolated from Toxic Clams and Mussels. *J. Am. Chem. Soc.* **1957**, *79*, 5235–5238. [CrossRef]
38. Schuett, W.; Rapoport, H. Saxitoxin, the Paralytic Shellfish Poison. Degradation to a Pyrrolopyrimidine. *J. Am. Chem. Soc.* **1962**, *84*, 2266–2267. [CrossRef]
39. Russell, F.E. Comparative pharmacology of some animal toxins. *Fed. Proc.* **1967**, *26*, 1206–1224.
40. Bordner, J.; Thiessen, W.E.; Bates, H.A.; Rapoport, H. Structure of a crystalline derivative of saxitoxin. Structure of saxitoxin. *J. Am. Chem. Soc.* **1975**, *97*, 6008–6012. [CrossRef]
41. Rogers, P.S.; Rapoport, H. The pKa's of saxitoxin. *J. Am. Chem. Soc.* **1980**, *102*, 7335–7339. [CrossRef]
42. Henderson, R.; Ritchie, J.M.; Strichartz, G.R. Evidence that tetrodotoxin and saxitoxin act at a metal cation binding site in the sodium channels of nerve membrane. *Proc. Natl. Acad. Sci. USA* **1974**, *71*, 3936–3940. [CrossRef] [PubMed]
43. Hille, B. The receptor for tetrodotoxin and saxitoxin. A structural hypothesis. *Biophys. J.* **1975**, *15*, 615–619. [PubMed]
44. Pan, X.; Li, Z.; Zhou, Q.; Shen, H.; Wu, K.; Huang, X.; Chen, J.; Zhang, J.; Zhu, X.; Lei, J.; et al. Structural basis for the modulation of voltage-gated sodium channels by animal toxins. *Science* **2018**, *362*, eaau2596.
45. Shen, H.; Liu, D.; Wu, K.; Lei, J.; Yan, N. Structures of human $Na_V1.7$ channel in complex with auxiliary subunits and animal toxins. *Science* **2019**, *363*, 1303–1308. [CrossRef] [PubMed]
46. Walker, J.R.; Novick, P.A.; Parsons, W.H.; McGregor, M.; Zablocki, J.; Pande, V.S.; Du Bois, J. Marked difference in saxitoxin and tetrodotoxin affinity for the human nociceptive voltage-gated sodium channel ($Na_V1.7$). *Proc. Natl. Acad. Sci. USA* **2012**, *109*, 18102–18107. [CrossRef]
47. Thomas-Tran, R.; Du Bois, J. Mutant cycle analysis with modified saxitoxins reveals specific interactions critical to attaining high-affinity inhibition of $hNa_V1.7$. *Proc. Natl. Acad. Sci. USA* **2016**, *113*, 5856–5861. [CrossRef]
48. Wiese, M.; D'Agostino, P.M.; Mihali, T.K.; Moffitt, M.C.; Neilan, B.A. Neurotoxic Alkaloids: Saxitoxin and Its Analogs. *Mar. Drugs* **2010**, *8*, 2185–2211. [CrossRef]

49. Yotsu-Yamashita, M.; Kim, Y.H.; Dudley, S.C., Jr.; Choudhary, G.; Pfahnl, A.; Oshima, Y.; Daly, J.W. The structure of zetekitoxin AB, a saxitoxin analog from the Panamanian golden frog Atelopus zeteki: A potent sodium-channel blocker. *Proc. Natl. Acad. Sci. USA* **2004**, *101*, 4346–4351. [CrossRef]
50. Fuhrman, F.A.; Fuhrman, G.J.; Mosher, H.S. Toxin from Skin of Frogs of the Genus Atelopus: Differentiation from Dendrobatid Toxins. *Science* **1969**, *165*, 1376–1377. [CrossRef]
51. Shindelman, J.; Mosher, H.S.; Fuhrman, F.A. Atelopidtoxin from the Panamanian frog, Atelopus Zeteki. *Toxicon* **1969**, *7*, 315–319. [CrossRef]
52. Tanino, H.; Nakada, T.; Kaneko, Y.; Kishi, Y. A stereospecific total synthesis of dl-saxitoxin. *J. Am. Chem. Soc.* **1977**, *99*, 2818–2819. [CrossRef] [PubMed]
53. Jacobi, P.A.; Martineli, M.J.; Polanc, S. Total synthesis of (±)-saxitoxin. *J. Am. Chem. Soc.* **1984**, *106*, 5594–5598. [CrossRef]
54. Fleming, J.J.; Du Bois, J. A Synthesis of (+)-Saxitoxin. *J. Am. Chem. Soc.* **2006**, *128*, 3926–3927. [CrossRef]
55. Iwamoto, O.; Koshino, H.; Hashizume, D.; Nagasawa, K. Total synthesis of (−)-decarbamoyloxysaxitoxin. *Angew. Chem. Int. Ed.* **2007**, *46*, 8625–8628. [CrossRef]
56. Mulcahy, J.V.; Du Bois, J. A Stereoselective Synthesis of (+)-Gonyautoxin 3. *J. Am. Chem. Soc.* **2008**, *130*, 12630–12631. [CrossRef]
57. Iwamoto, O.; Shinohara, R.; Nagasawa, K. Total Synthesis of (−)- and (+)-Decarbamoyloxysaxitoxin and (+)-Saxitoxin. *Chem. Asian J.* **2009**, *4*, 277–285. [CrossRef]
58. Iwamoto, O.; Nagasawa, K. Total Synthesis of (+)-Decarbamoylsaxitoxin and (+)-Gonyautoxin 3. *Org. Lett.* **2010**, *12*, 2150–2153. [CrossRef]
59. Sawayama, Y.; Nishikawa, T. A Synthetic Route to the Saxitoxin Skeleton: Synthesis of Decarbamoyl α-Saxitoxinol, an Analogue of Saxitoxin Produc ed by the Cyanobacterium Lyngbya wollei. *Angew. Chem. Int. Ed.* **2011**, *50*, 7176–7178. [CrossRef]
60. Bhonde, V.R.; Looper, R.E. A Stereocontrolled Synthesis of (+)-Saxitoxin. *J. Am. Chem. Soc.* **2011**, *133*, 20172–20174. [CrossRef]
61. Mulcahy, J.V.; Walker, J.R.; Merit, J.E.; Whitehead, A.; Du Bois, J. Synthesis of the Paralytic Shellfish Poisons (+)-Gonyautoxin 2, (+)-Gonyautoxin 3, and (+)-11,11-Dihydroxysaxitoxin. *J. Am. Chem. Soc.* **2016**, *138*, 5994–6001. [CrossRef] [PubMed]
62. Thottumkara, A.P.; Parsons, W.H.; Du Bois, J. Saxitoxin. *Angew. Chem. Int. Ed.* **2014**, *53*, 5760–5784. [CrossRef] [PubMed]
63. Andresen, B.M.; Du Bois, J. De Novo Synthesis of Modified Saxitoxins for Sodium Ion Channel Study. *J. Am. Chem. Soc.* **2009**, *131*, 12524–12525. [CrossRef] [PubMed]
64. Parsons, W.H.; Du Bois, J. Maleimide Conjugates of Saxitoxin as Covalent Inhibitors of Voltage-Gated Sodium Channels. *J. Am. Chem. Soc.* **2013**, *135*, 10582–10585. [CrossRef]
65. Akimoto, T.; Masuda, A.; Yotsu-Mari, M.; Hirokawa, T.; Nagasawa, K. Synthesis of saxitoxin derivatives bearing guanidine and urea groups at C13 and evaluation of their inhibitory activity on voltage-gated sodium channels. *Org. Biomol. Chem.* **2013**, *11*, 6642–6649. [CrossRef]
66. Arakawa, O.; Nishio, S.; Noguchi, T.; Shida, Y.; Onoue, Y. A new saxitoxin analogue from a xanthid crab Atergatis Floridus. *Toxicon* **1995**, *12*, 1577–1584. [CrossRef]
67. Wang, C.; Oki, M.; Nishikawa, T.; Harada, D.; Yotsu-Yamashita, M.; Nagasawa, K. Total Synthesis of 11-Saxitoxinethanoic Acid and Evaluation of its Inhibitory Activity on Voltage-gated Sodium Channels. *Angew. Chem. Int. Ed.* **2016**, *55*, 11600–11603. [CrossRef]
68. Walker, R.J.; Merit, E.J.; Thomas-Tran, R.; Tang, D.T.Y.; Du Bois, J. Divergent Synthesis of Natural Derivatives of (+)-Saxitoxin Including 11-Saxitoxinethanoic Acid. *Angew. Chem. Int. Ed.* **2018**, *58*, 1689–1693. [CrossRef]
69. Paladugu, S.R.; James, C.K.; Looper, R.E. A Direct C11 Alkylation Strategy on the Saxitoxin Core: A Synthesis of (+)-11-Saxitoxinethanoic Acid. *Org. Lett.* **2019**, *21*, 7999–8002. [CrossRef]
70. Lou, J.-Y.; Laezza, F.; Gerber, B.R.; Xiao, M.L.; Yamada, K.A.; Hartmann, H.; Craig, A.M.; Nerbonne, J.M.; Ornitz, D.M. Fibroblast growth factor 14 is an intracellular modulator of voltage-gated sodium channels. *J. Physiol.* **2005**, *569*, 179–193. [CrossRef]
71. Matsuo, J.; Murakami, M. The Mukaiyama Aldol Reaction: 40 Years of Continuous Development. *Angew. Chem. Int. Ed.* **2013**, *52*, 9109–9118. [CrossRef] [PubMed]

72. Mase, N.; Hayashi, Y. The Aldol Reaction: Organocatalysis Approach. In *Comprehensive Organic Synthesis*, 2nd ed.; Knochel, P., Molander, G.A., Eds.; Elsevier: Amsterdam, The Netherlands, 2014; Volume 2, pp. 273–339.
73. Hosokawa, S. Recent development of vinylogous Mukaiyama aldol reactions. *Tetrahedron Lett.* **2018**, *59*, 77–88. [CrossRef]
74. Mukaiyama, T.; Narasaka, K.; Banno, K. New aldol type reaction. *Chem. Lett.* **1973**, 1011–1014.
75. Mukaiyama, T.; Banno, K.; Narasaka, K. New cross-aldol reactions. Reactions of silyl enol ethers with carbonyl compounds activated by titanium tetrachloride. *J. Am. Chem. Soc.* **1974**, *96*, 7503–7509. [CrossRef]
76. Noyori, R.; Yokoyama, K.; Sakata, J.; Kuwajima, I.; Nakamura, E.; Shimizu, M. Fluoride ion catalyzed aldol reaction between enol silyl ethers and carbonyl compounds. *J. Am. Chem. Soc.* **1977**, *99*, 1265–1267. [CrossRef]
77. Gingras, M.; Chabre, Y.M.; Raimundo, J.-M. Tetrabutylammonium Difluorotriphenylstannate [Bu_4N][Ph_3SnF_2]: Delivering Carbon or Fluorine Ligands via Hypercoordination. *Synthesis* **2006**, *1*, 182–185. [CrossRef]
78. Hama, T.; Liu, X.; Culkin, D.A.; Hartwig, J.F. Palladium-Catalyzed α-Arylation of Esters and Amides under More Neutral Conditions. *J. Am. Chem. Soc.* **2003**, *125*, 11176–11177. [CrossRef]
79. Moradi, W.A.; Buchwald, S.L. Palladium-Catalyzed α-Arylation of Esters. *J. Am. Chem. Soc.* **2001**, *123*, 7996–8002. [CrossRef]
80. Magauer, T.; Mulzer, J.; Tiefenbacher, K. Total Syntheses of (+)-Echinopine A and B: Determination of Absolute Stereochemistry. *Org. Lett.* **2009**, *11*, 5306–5309. [CrossRef]
81. Xiao, Q.; Ren, W.-W.; Chen, Z.-X.; Sun, T.-W.; Li, Y.; Ye, Q.-D.; Gong, J.-X.; Meng, F.-K.; You, L.; Liu, Y.-F.; et al. Diastereoselective Total Synthesis of (±)-Schindilactone A. *Angew. Chem. Int. Ed.* **2011**, *50*, 7373–7377. [CrossRef]
82. Negishi, E. Novel and selective α-substitution of ketones and other carbonyl compounds based on Pd-catalyzed cross coupling of α-unsaturated carbonyl derivatives containing α-halogen or α-metal groups. *J. Organomet. Chem.* **1999**, *576*, 179–194. [CrossRef]
83. Johnson, C.R.; Adams, J.P.; Braun, M.P.; Senanayake, C.B.W. Modified stille coupling utilizing α-iodoenones. *Tetrahedron Lett.* **1992**, *33*, 919–922. [CrossRef]
84. Cordvilla, C.; Bartolome, C.; Martinez-Ilarduya, J.M.; Espinet, P. The Stille Reaction, 38 Years Later. *ACS Catal.* **2015**, *5*, 3040–3053. [CrossRef]
85. Han, X.; Stoltz, B.; Corey, E.J. Cuprous Chloride Accelerated Stille Reactions. A General and Effective Coupling System for Sterically Congested Substrates and for Enantioselective Synthesis. *J. Am. Chem. Soc.* **1999**, *121*, 7600–7605. [CrossRef]
86. Devlin, A.S.; Du Bois, J. Modular synthesis of the pentacyclic core of batrachotoxin and select batrachotoxin analogue designs. *Chem. Sci.* **2013**, *4*, 1059–1063. [CrossRef] [PubMed]
87. Allred, G.D.; Liebeskind, L.S. Copper-Mediated Cross-Coupling of Organostannanes with Organic Iodides at or below Room Temperature. *J. Am. Chem. Soc.* **1996**, *118*, 2748–2749. [CrossRef]
88. Colomer, I.; Velado, M.; Fe rnandez de la Pradilla, R.; Viso, A. From Allylic Sulfoxides to Allylic Sulfenates: Fifty Years of a Never-Ending [2,3]-Sigmatropic Rearrangement. *Chem. Rev.* **2017**, *117*, 14201–14243. [CrossRef]
89. Rojas, C.M. The Mislow-Evans rearrangement. In *Molecular Rearrangements in Organic Synthesis*; Rojas, C.M., Ed.; John Wiley & Sons: Hoboken, NJ, USA, 2016. [CrossRef]
90. Johnson, C.R.; Adams, J.P.; Braun, M.P.; Senanayake, C.B.W.; Wovkulich, P.M.; Uskokovic, M.R. Direct α-iodination of cycloalkenones. *Tetrahedron Lett.* **1992**, *33*, 917–918. [CrossRef]
91. Djuardi, E.; Bovonsombat, P.; McNelis, E. Formations of α-Iodoenones by Iodine and Catalytic Amounts of Amines. *Synth. Commun.* **1997**, *27*, 2497–2503. [CrossRef]
92. Adachi, K.; Yamada, T.; Ishizuka, H.; Oki, M.; Tsunogae, S.; Shimada, N.; Chiba, O.; Orihara, T.; Hidaka, M.; Hirokawa, T.; et al. Synthesis of C12-keto saxitoxin derivatives with unusual inhibitory activity against voltage-gated sodium channels. *Chem. Eur. J.* **2019**. [CrossRef]
93. Nishikawa, T.; Urabe, D.; Isobe, M. Syntheses of *N*-Acylisoxazolidine Derivatives, Related to a Partial Structure Found in Zetekitoxin AB, a Golden Frog Poison. *Heterocycles* **2009**, *79*, 379–385. [CrossRef]
94. Paladugu, S.R.; Looper, R.E. Preparation of a 1,2-isoxazolidine synthon for the synthesis of zetekitoxin AB. *Tetrahedron Lett.* **2015**, *56*, 6332–6334. [CrossRef] [PubMed]

95. Bernet, B.; Vasella, A. Carbocyclische Verbindungen aus Monosacchariden. II. Umsetzungen in der Mannosereihe. *Helv. Chim. Acta* **1979**, *62*, 2400–2410. [CrossRef]
96. Ferrier, R.J.; Furneaux, R.H.; Prasit, P.; Tyler, P.C. Functionalised carbocycles from carbohydrates. Part 2. The synthesis of 3-oxa-2-azabicyclo[3.3.0]octanes. X-Ray crystal structure of (1*R*,5*S*)-6-*exo*,7-*endo*,8-*exo*-triacetoxy-*N*-methyl-4-*endo*-phenylthio-3-oxa-2-azabicyclo[3.3.0]octane. *J. Chem. Soc. Perkin Trans. 1* **1983**, *1*, 1621–1628. [CrossRef]
97. Dransfield, P.J.; Moutel, S.; Shipman, M.; Sik, V. Stereocontrolled synthesis of polyhydroxylated hexahydro-1*H*-cyclopent[*c*]isoxazoles by intramolecular oxime olefin cycloadditions: An approach to aminocyclopentitols. *J. Chem. Soc. Perkin Trans. 1* **1999**, *1*, 3349–3355. [CrossRef]
98. Ogawa, S.; Orihara, M. Synthesis of the penta-*N*,*O*-acetyl derivatives of some pseudo-3-amino-3-deoxy-DL-hexopyranoses a and -DL-hexopyranosylamine derivative. *Carbohydr. Res.* **1989**, *189*, 323–330. [CrossRef]
99. Baumgartner, H.; O'Sullivan, A.C.; Schneider, J. The Synthesis of Oxa-Analogs of the Kainoid Family. *Heterocycles* **1997**, *45*, 1537–1549.
100. Nishikawa, T.; Wang, C.; Akimoto, T.; Koshino, H.; Nagasawa, K. Synthesis of an advance model of zetekitoxin AB focusing on *N*-acylisoxazolidine amide structure corresponding to C13–C17. *Asian J. Org. Chem.* **2014**, *3*, 1308–1311. [CrossRef]
101. Shibuya, M.; Tomizawa, M.; Suzuki, I.; Iwabuchi, Y. 2-Azaadamantane *N*-Oxyl (AZADO) and 1-Me-AZADO: Highly Efficient Organocatalysts for Oxidation of Alcohols. *J. Am. Chem. Soc.* **2006**, *128*, 8412–8413. [CrossRef]
102. Shibuya, M.; Sato, T.; Tomizawa, M.; Iwabuchi, Y. Oxoammonium salt/$NaClO_2$: An expedient, catalytic system for one-pot oxidation of primary alcohols to carboxylic acids with broad substrate applicability. *Chem. Commun.* **2009**, *13*, 1739–1741. [CrossRef]
103. Kunishima, M.; Kawachi, C.; Hioki, K.; Tani, S. Formation of carboxamides by direct condensation of carboxylic acids and amines in *alcohols* using a new alcohol- and water-soluble condensing agent: DMT-MM. *Tetrahedron* **2001**, *57*, 1551–1558. [CrossRef]

© 2019 by the authors. Licensee MDPI, Basel, Switzerland. This article is an open access article distributed under the terms and conditions of the Creative Commons Attribution (CC BY) license (http://creativecommons.org/licenses/by/4.0/).